

Probing the effect of electron donation on CO₂ absorbing 1,2,3-triazolide ionic liquids†

 Cite this: *RSC Adv.*, 2014, 4, 12748

 Robert L. Thompson,^{*ab} Wei Shi,^{ab} Erik Albenze,^{ab} Victor A. Kusuma,^a David Hopkinson,^a Krishnan Damodaran,^c Anita S. Lee,^d John R. Kitchin,^d David R. Luebke^a and Hunaid Nulwala^{*ae}

Development of the next generation materials for effective separation of gases is required to address various issues in energy and environmental applications. Ionic liquids (ILs) are among the most promising material types. To overcome the many hurdles in making a new class of materials technologically applicable, it is necessary to identify, access, and scale up a range of representative substances. In this work, CO₂ reactive triazolide ILs were synthesized and characterized with the aim of developing a deeper understanding of how structural changes affect the overall properties of these substances. It was found that substituents on the anion play a crucial role in dictating the physical properties for CO₂ capture. Depending upon the anion substituent, CO₂ capacities between 0.07 and 0.4 mol CO₂ per mol IL were observed. It was found that less sterically-hindered anions and anions containing electron donating groups were more reactive towards CO₂. Detailed spectroscopic, CO₂ absorption, rheological, and simulation studies were carried out to understand the nature and influence of these substituents. The effect of water content was also evaluated, and it was found that water had an unexpected impact on the properties of these materials, resulting in an increased viscosity, but little change in the CO₂ reactivity.

 Received 27th November 2013
 Accepted 17th February 2014

DOI: 10.1039/c3ra47097k

www.rsc.org/advances

Introduction

In addition of their novel physical properties, the diversity and adaptability of ionic liquids (ILs) makes them attractive to materials scientists seeking to create the ideal material for a particular application.¹ The requirements for CO₂ capture solvents in current and advanced fossil-based power systems are considerable.^{2–8} If a truly superior material is to be located, the thermal stability, low flammability, high CO₂ solubility, and extremely low vapor pressure which are characteristic of many IL types will be important, but the ability to tailor the structure and properties of the final substance to optimize them for the application will be indispensable.^{9–15} CO₂-reactive ILs will be the focus of this study since they are well-suited to address the most immediate need in global climate change mitigation, capture of CO₂ from existing power plants.^{16,17}

In the case of CO₂-reactive ILs, the presence of hydrogen atoms on the anion which are available for hydrogen bonding is suspected of leading to high viscosities through the formation of salt-bridges.¹⁸ It was shown that this salt-bridge formation can be avoided by developing aprotic heterocyclic anions (AHA) which lack the necessary proton to form salt bridges as reported by Wang.^{11,19,20} These AHA ILs may then be used to efficiently and reversibly capture CO₂ in equimolar stoichiometry without the increase in viscosity.^{21,22} The new ILs can be prepared from simple azoles and can be tuned for stability, CO₂ absorption enthalpy, and CO₂ capacity based on the choice of the azole.^{11,12,23–25}

The pK_a for a given 1,2,3-triazole typically falls within the range useful in carbon capture, with the pK_a of 1,2,3-triazole being 13.9. Another benefit of this class of AHA ILs is the ease of access to substituted 1,2,3-triazoles which can be assembled by a facile Cu(I) catalyzed click reaction (Scheme 1) resulting in a region-specific 1,4-disubstituted triazole.^{13,15} The ability to evaluate a variety of functional groups at specific locations on the triazole ring associated with this chemistry is highly valuable, allowing evaluation of both steric and electronic effects on the properties of the final IL. A set of substituted triazolide based AHA ILs containing the tetrabutyl phosphonium cation were synthesized. The anions prepared are illustrated in Fig. 1. The synthetic details for these ILs were reported previously.¹⁰

In this combined experimental and computational study, we show that by varying the electronic nature of the substituent at the 4-position on the triazole ring, stabilization of the negative

^aU.S. Dept. Of Energy, National Energy Technology Laboratory, 626 Cochrans Mill Rd., Pittsburgh, PA 15236, USA. E-mail: robert.thompson@contr.netl.doe.gov; Tel: 1-412-386-4953

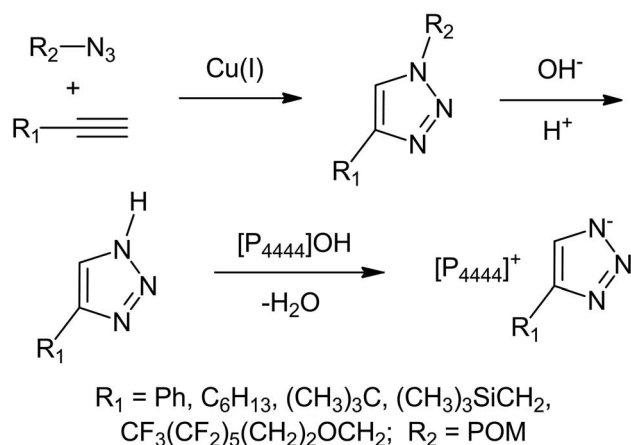
^bURS Corporation, P.O. Box 618, South Park, PA 15129, USA

^cUniversity of Pittsburgh, Department of Chemistry, Pittsburgh, PA 15260, USA

^dCarnegie Mellon University, Department of Chemical Engineering, Pittsburgh, PA 15213, USA

^eCarnegie Mellon University, Department of Chemistry, Pittsburgh, PA 15213, USA. E-mail: hnulwala@andrew.cmu.edu; Tel: +1-412-386-7343

† Electronic supplementary information (ESI) available. See DOI: 10.1039/c3ra47097k



Scheme 1

charge on the resulting anion can be affected, having a significant impact on the overall properties.

Experimental

General information

The ^1H , ^{13}C , ^{19}F , and ^{31}P NMR spectroscopic analyses were completed using Bruker Avance III 300 or 400 MHz spectrometer. Fourier transform infrared (FTIR) spectra were collected on a Nicolet Spectrum 100 with an attenuated total reflectance (ATR) apparatus. Density measurements of the ILs were performed using a Micromeritics Accupyc II 1340 pycnometer. Water content was determined using a Metrohm 860 Karl Fisher (KF) Thermoprep titration unit, equipped with an 831 KF Coulometer; IL samples which had undergone KF titration were treated as water-free samples. Viscosity measurements were made at ambient temperatures (22–24 °C) using a Rheosense Inc. μVisc unit and 400 μL pipettes.

Thermogravimetric analysis

Thermal decomposition studies were performed on a Mettler Toledo TGA/DSC 1 STARE System, equipped with a GC 200 gas controller. Thermal decompositions were conducted under N_2 purge from 22 °C to 500 °C at a ramp rate of 10 °C per minute. The onset of thermal decomposition (T_{onset}) was evaluated as the temperature at which the signal baseline began to drop to a value exceeding that observed in the preceding baseline noise.

Mass spectrometry analysis

Mass spectrometry (MS) analysis was performed using an Agilent 1290 LC system and 6520 Q-TOF (quadrupole time of flight) detector (Agilent Technology). A 95% MeOH–5% H_2O mixture was used as the mobile phase. A 0.1 μL sample was injected using an autosampler and introduced into the chromatograph using direct infusion (no column) with a mobile phase flow rate of 0.4 mL min^{-1} . An ESI (electrospray ionization) source was used to introduce the samples into the Q-TOF with the following settings: fragmentor voltage = 175 V, skimmer voltage = 65 V, drying gas flow rate and temperatures of 12 L min^{-1} and 300 °C,

respectively. The acquisition range was 100–3000 m/z with a scanning rate of 1.03 spectra per s. Each sample was run for 4 min in both positive and negative polarities. MeOH blanks were run between injections to decrease the amount of carryover that may occur. The chromatograms were integrated and extracted for MS spectra to determine the masses of the cations and anions.

FTIR spectroscopy

Variable pressure FTIR experiments performed were conducted on a Nicolet Nexus 6700 ESP spectrometer (Thermo Fisher Scientific, Waltham, MA), equipped with a wide-band mercury cadmium telluride (MCT) detector cooled by liquid N_2 . Low pressure infrared studies were performed in a stainless steel vacuum chamber equipped with a turbo-molecular pump, roughing pump, precision leak valve, and differentially pumped optical windows (KBr). System pressure was measured using an ionization gauge. The system base pressure was in the 10^{-7} mbar range after an overnight evacuation. The sample was manipulated inside the chamber with an XYZ translation stage and a rotation stage. Samples were prepared on CaF_2 windows using a Janis Research (Wilmington, MA) copper sample holder, accommodating one blank and one sample window.

CO_2 absorption

Gas solubility measurements were performed using a PCT-Pro 2000 apparatus from Setaram Inc. The PCT-Pro 2000 is a Sievert's apparatus which determines gas solubility in a sample by charging a sealed sample chamber of known volume with a known quantity of CO_2 . The CO_2 -charged sample chamber is isolated from the rest of the system and the pressure drop in the chamber is measured. The drop in pressure due to CO_2 absorption into the liquid is then measured, and the quantity of CO_2 absorbed into the liquid is determined from an equation of state listed in the NIST Standard Reference Database 23.^{26,27}

For all tests, between 0.2 g and 0.4 g of sample was loaded into the sample chamber. The sample was held under a dynamic vacuum for 4 hours prior to starting a test. During this evacuation, the sample was heated to 30 °C and was stirred at 300 rpm. After evacuation, testing was initiated by dosing the sample chamber with a known amount of CO_2 , and the sample was allowed to equilibrate for at least 4 hours. Dosing was repeated to obtain an isotherm over a pressure range of 0 to 10 bar. Throughout all tests, the sample was maintained at 30 °C and was stirred at 300 rpm.

CO_2 absorption was also measured using a Thermo Scientific Thermax 500 TGA. A sample volume of 50 cm^3 was used with a constant temperature of 40 °C and pressure of 0.9 bar. The sample was exposed to pure N_2 under a constant flow rate of 0.1 SLPM for several days until it reached an equilibrium mass. An initial decrease in mass was observed due to evaporation of water from the sample and the surface of the sample bucket. Next the feed gas was switched to pure CO_2 at a flow rate of 0.1 SLPM and was allowed approximately one day to reach equilibrium as CO_2 absorbed into the sample. The difference between these two equilibrium masses was considered to be the amount of CO_2 absorbed by the sample.

Theoretical calculations

Ab initio gas-phase calculations were performed at the B3LYP/6-311++g(d,p) level of theory to calculate CO₂ interactions with anions on different binding sites of the same anions. The interaction energy was calculated as the energy difference between the products and the reactants (CO₂ and anions) corresponding to the respective optimized structures. Vibrational frequency calculations were performed to confirm minimum stable energy structures for both the reactants and the products. Reaction enthalpies of CO₂ with anions were also calculated at 298 K. The reaction enthalpy includes the total electronic energy, zero point energy, thermal corrections to 298 K using the standard ideal gas statistical mechanics formulation, and *PV* (*RT*) energy. The charges for atoms of the anions were obtained from the CHELPG protocol;²⁸ all calculations were performed using the Gaussian 09 program.²⁹ The water interactions with the anions were calculated in a similar fashion to CO₂. In the case of water, we used counterpoise correction in both the structural optimization and frequency calculations.

Materials

Unless otherwise stated, ACS reagent grade chemicals and solvents were obtained from Aldrich and used as received. Tetrabutyl phosphonium hydroxide (40% aqueous solution) was obtained from TCI America and was used as received.

Syntheses of ionic liquids (1–5)

The details for the preparation of the ILs studied in this work, which are shown in Fig. 1 are described in the ESI,[†] and were published previously.¹⁰

Results and discussion

The structures of the triazoles prepared are shown in Fig. 1. Triazole targets were chosen to include electron-withdrawing (phenyl – 1) and electron-donating (hexyl and *tert*-butyl – 2, 3)

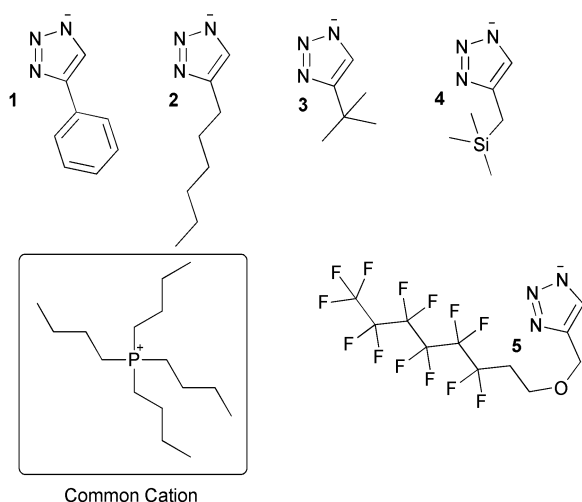


Fig. 1 Tetrabutyl phosphonium 4-substituted-1,2,3-triazolide IL anions 1–5 prepared and studied in this work.

Table 1 Physical properties of ILs 1–5

IL	FW, g mol ⁻¹	Density, g mL ⁻¹	<i>T</i> _{onset} , °C	wt% H ₂ O (by KF) ^a	mol% H ₂ O (by KF) ^a
1	403.58	0.9836	238	1.06	23.7
2	411.65	0.9324	185	2.35	53.7
3	383.59	0.9290	151	0.914	19.5
4	413.70	0.9400	227	1.04	23.9
5	704.61	1.2141	263	0.973	38.0

^a Water content after drying to constant weight at 50 °C.

Table 2 CO₂ absorption capacities of ILs 1–5

IL	mol CO ₂ per mol IL absorbed ^a	<i>θ</i> PR ₃ , ° (ref. 33)	<i>δ</i> H ₅ , ppm
1	0.10	145° (Ph)	7.59
2	0.40	132° (<i>n</i> Bu)	7.23
3	0.07	182° (<i>t</i> Bu)	7.12
4	0.30	180° (CH ₂ <i>t</i> Bu)	7.16
5	0.23	132° (<i>n</i> Bu)	7.36

^a CO₂ absorptions as determined at 30 °C and 1 atm.

groups at the 4-position. Silyl- and fluorinated ether-substituted triazoles (4, 5) were also included to observe the effect of hydrophobic substituents on the IL.

All five 1,2,3-triazoles were converted into ILs *via* a dehydration reaction with aqueous tetrabutyl phosphonium hydroxide. The density, water content, and onset of thermal decomposition of the resulting ILs were measured and the results are listed in Table 2. The densities of all of the ILs except for the fluorinated 5 were approximately 1 g mL⁻¹. All ILs were vacuum dried to constant weight at 50 °C, but KF titration of these samples showed that significant moisture was retained in the vacuum dried ILs as shown in Table 1.

Thermal decomposition analysis³⁰ of ILs 1–5 showed that ILs with electron donating groups on the triazole ring began to decompose at lower temperatures than those with electron withdrawing groups (Table 1). Alkyl groups on 2 and 3 cause the ILs to begin thermal decomposition at a substantially lower temperature than 1 and 5, presumably due to more efficient electron donation to the anion. The thermal decomposition temperatures under N₂ as measured by TGA for 1–5 were found to be comparable with results reported by Wang for both [P₆₆₆₁₄]-[imidazolide] and [P₆₆₆₁₄][pyrazolide].¹¹

The results for the CO₂ solubility experiments are summarized in Fig. 2 and Table 2, and the data for these experiments is listed in ESI Tables 2 and 10.[†] The CO₂ capacity at 1 bar and 30 °C was shown to vary from 0.07 mol CO₂ per mol IL in the case of 3 to as high as 0.40 mol CO₂ per mol IL in the case of 2. For comparison, the amount of CO₂ physisorbed by [hmim]-[Tf₂N] under identical conditions is 0.032 mol CO₂ per mol IL.^{31,32} CO₂ absorption experiments were also performed by TGA for 1 under comparable conditions, but the long equilibration times required by the TGA (1–2 days) and the ability of the Sievert's apparatus to stir samples led us to not pursue the TGA for further studies (ESI Table 10[†]).

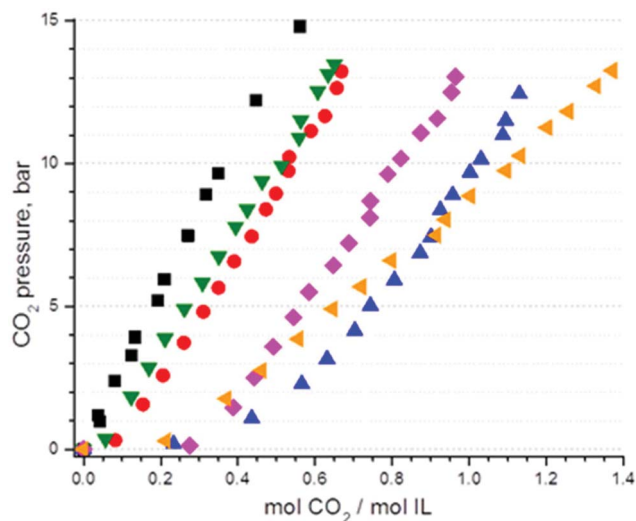


Fig. 2 CO₂ solubility in ILs 1–5 and [hmim][Tf₂N] at 30 °C as determined by Sievert's apparatus. Filled squares indicate data for [hmim][Tf₂N], circles for 1, upwards triangles for 2, downwards triangles for 3, diamonds for 4, and leftwards triangles for 5.

From the results obtained, it can be inferred that the steric bulk of the substituent combined with their electron donating or withdrawing nature plays a significant role in CO₂ solubility. In the cases of 2 and 5, the linear geometry of the hexyl- and fluoroether-groups exhibit less steric crowding adjacent to the azole ring, leaving the incoming CO₂ a greater amount of free space in which to react. In the case of 3, the branched nature of the *tert*-butyl group maximizes the steric crowding near the azole ring and prevents the CO₂ from having an easy approach during reaction. IL 4 (TMSCH₂ – electron donating group) has a greater CO₂ capacity than 1 (Ph – electron withdrawing group) suggesting that while steric crowding is an important factor in determining CO₂ capacity, electronic effects have a much larger influence on the CO₂ reaction.

One method for quantifying the relative steric crowding near the triazolide ring is the angular spread of the phosphine cone angle in comparable trialkyl phosphines (see Table 2).³³ The cone angle is smaller for straight chain substituents (132° for 2 and 5), indicating less steric crowding, and grows larger for the bulkier, highly-branched substituents (180–182° for 3 and 4). The cone angle for phenyl rings lies approximately half way between the linear and branched alkyl groups (145° for 1). All these observations are consistent with the assertion that sterics as well as electronics play a role in CO₂ absorption.

The relative effect of electron donating and withdrawing substitution at the 4-position is also observed in the ¹H NMR by monitoring the chemical shift of the triazole ring proton at the 5-position. The shifts in the 1,2,3-triazolides with electron donating groups (ILs 2, 3, and 4 with shifts of 7.12–7.23 ppm in CDCl₃) are observed upfield from those of the ILs with electron withdrawing groups, (ILs 1 and 5 with shifts of 7.36–7.59 ppm), reflecting the less shielded environment for the protons in the latter cases. Related effects are also reflected in the relative chemical shifts for the H₅ proton in the parent 1H-1,2,3-triazoles and in the 1,2,3-triazolide ILs, listed in ESI Table 3.† The H₅ NMR signal shifted

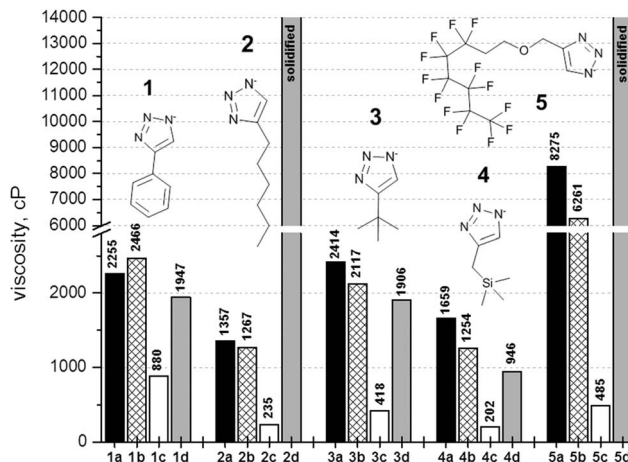


Fig. 3 Viscosity of ILs 1–5, as determined at ambient temperature. ILs 1–5 were tested wet and dry, both with and without CO₂ added. Samples labeled a (black) are wet (dried to constant weight), b (hatched) are wet + CO₂, c (white) are dry (KF titrated), and d (grey) are dry + CO₂.

upfield 0.1–0.4 ppm for all five triazoles after conversion to ILs, indicating that the electronic environment of the azole ring was more electron-rich after converting to anionic form.

The viscosities of the 1,2,3-triazolide ILs were determined in both wet and dry samples, both before and after exposure to CO₂; these results are illustrated in Fig. 3 at room temperature (see data in ESI Tables 4 and 5†) The water content of each sample is shown in Table 1. Samples listed as dry were further treated by subjecting them to KF titration and thus contain less than 100 ppm H₂O (detection limit of KF titration at 120 °C). Both wet and dry IL samples 1–5 were later exposed to 1 bar CO₂ by evacuating them on a Schlenk line and backfilling with CO₂ for 1 h while heating at 50 °C, then cooling to room temperature.

The wet IL samples were relatively high in viscosity, ranging from 1357 cP (2) to 8275 cP (5), and did not show any substantial change in viscosity after exposure to CO₂ (see Fig. 3). The dried IL samples were significantly lower in viscosity, ranging from 202 cP (4) to 880 cP (1), but unexpectedly increased significantly in viscosity after CO₂ exposure. Comparison of wet and dry IL viscosities suggests that water molecules were able to interact strongly with the anions to form a hydrogen-bonding network, which leads to high viscosities for the wet ILs (compare experimental water content values in Table 1 with viscosities in ESI Tables 4 and 5†).^{34,35} Thus, when CO₂ was added to the wet ILs, which already have a hydrogen bonding network in place, no further effect on the viscosity was observed. When CO₂ was added to the dry ILs, where no network previously existed, CO₂ absorption caused viscosities to increase by increasing the overall molecular weight of the anion, despite the lack of hydrogen bonding sites on the azole rings. It is also important to note that when exposed to CO₂ under absolutely dry conditions the reaction product was a solid for 2 and 5.

A comparison of the CO₂ solubility in wet and dry samples of 2 and 3 is shown in Fig. 4. The data (ESI Table 6†) show that there was no discernible difference in CO₂ absorption capacity in the presence of water with concentrations as high as 54 mole percent. Although water tends to increase IL viscosity at water contents

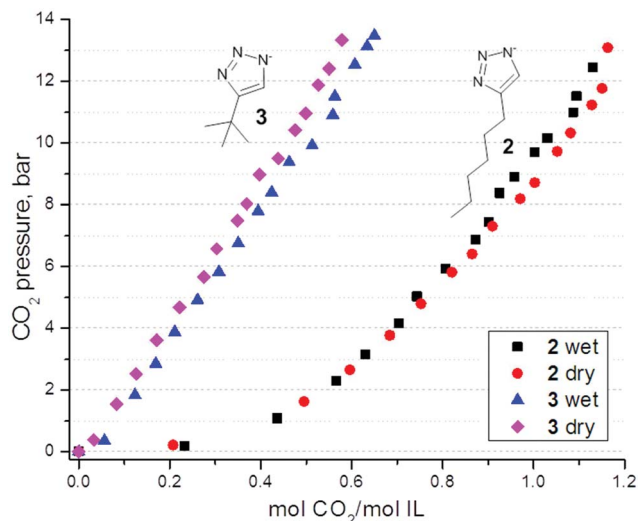
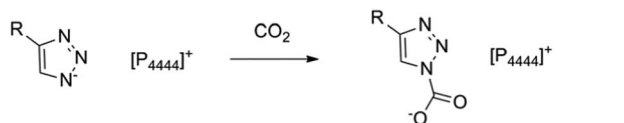


Fig. 4 CO₂ absorption by wet and dry IL samples 2 and 3 at 30 °C as determined by Sievert's apparatus. Filled circles indicate data for wet 2 (vacuum dried to constant weight at 50 °C), squares indicate data for dry 2 (KF titrated after vacuum drying), triangles for wet 3, and diamonds for dry 3.

Dry CO₂ uptake:



Wet CO₂ uptake:

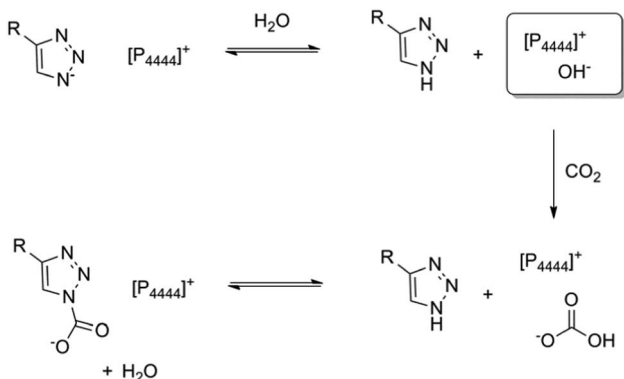


Fig. 5 Proposed CO₂ absorption mechanism by ILs under wet and dry conditions.

between 20 and 54 mole percent, the agitation caused by the stirring in the CO₂ absorption was adequate to overcome diffusion limitations, preventing any diminishing effect the moisture might exert on the CO₂ uptake through mass transport inhibition.

In the presence of water, we suspect that CO₂ uptake happens *via* a different mechanism. Our proposed mechanism is shown in Fig. 5 for CO₂ absorption in both the presence and absence of water. Fig. 5 shows that bicarbonate formation may result in very similar CO₂ uptake by utilizing a separate reaction pathway yielding approximately the same CO₂ content. In the

Table 3 ¹³C NMR chemical shifts before and after CO₂ exposure for neat ILs, 1–5^a

Sample	δ CO ₂ , ppm	δ C ₄ , ppm	δ C ₅ , ppm
1	—	141.3	133.9
1 + ¹³ CO ₂	158.1, 154.7	141.3	133.1
2	—	140.6	125.0
2 + ¹³ CO ₂	158.0, 154.6	140.6	124.9
3	—	150.9	122.9
3 + ¹³ CO ₂	157.9, 155.0	150.9	122.9
4	—	135.6	126.1
4 + ¹³ CO ₂	158.3, 155.0	135.6	126.1
5	—	138.5	126.2
5 + ¹³ CO ₂	159.0, 155.6, 153.6	138.5	128.3

^a Chemical shifts are normalized to untreated C₄.

Table 4 Mass spectral peaks for selected ions for methanol solutions of ILs 1–5^a

Sample		C ⁺	A ⁻	(2A + H) ⁻	(2A + C) ⁻
1	Calc.	259.43	144.15	289.31	547.73
	Expt.	259.26	144.07	nd	547.37
2	Calc.	259.43	152.22	305.45	563.87
	Expt.	259.26	152.12	305.24	563.49
3	Calc.	259.43	124.16	249.33	507.75
	Expt.	259.26	124.09	249.20	507.43
4	Calc.	259.43	154.27	309.55	567.97
	Expt.	259.26	154.10	nd	nd
5	Calc.	259.43	444.17	889.35	1147.77
	Expt.	259.26	444.04	889.13	1147.33

^a C = IL cation, A = IL anion, nd = not detected.

absence of water the CO₂ directly reacts with triazolide anion resulting in CO₂ adduct product. In the presence of water the reaction is perceived to be a combination of reactions including direct triazolide reaction to CO₂. The water can react with triazolide anion to form neutral triazole and OH⁻. The OH anion reaction with CO₂ would result in formation of [P₄₄₄₄][HCO₃]. The bicarbonate (pK_a = 10.3)²⁵ could further react with triazole to form the triazolide–CO₂ adduct.

The ¹³C NMR spectra of neat 1,2,3-triazolide ILs were all collected before and after exposure to ¹³CO₂. The two 1,2,3-triazolide ring carbons, labelled C₄ for the substituted site and C₅ for the protonated site, along with the new peaks attributed to addition of ¹³CO₂, are listed in Table 3 (see ESI Fig. 12–16†). As the spectra were recorded in neat solutions, there were no external reference peaks with which to compare, so all chemical shifts were normalized to the C₄ peak in the untreated IL samples. Extra ¹³C peaks were observed in the neat NMR spectra of 3 before and after ¹³CO₂ exposure, although they were not seen in the solution spectra. These may arise from the formation of anionic dimers (see below – Table 4); although theoretical studies have predicted that the protonated triazoles may have multiple tautomer structures accessible in solution.^{36,37} These extra peaks may also be caused by some fraction of the phosphonium cation being converted to ylide-form which could also be reactive towards CO₂.^{38,39}

The chemical shifts recorded for the ring carbons did not tend to change after CO₂ exposure, with only 5 showing a slight downfield shift of 2 ppm. However, two new signals were observed for 1 through 4, and three new signals were observed for 5 after exposure to CO₂. In every case, the new signals appeared between 153 and 159 ppm, which would be consistent with the formation of carbamate functional groups. The relative intensities of the new peaks are also consistent with their coming from an isotopically-enriched source, rather than the non-enriched IL signals. The new carbamate ¹³C NMR signals (153–159 ppm) for all five ¹³CO₂-treated AHA IL samples disappear upon dissolving them in d⁶-DMSO. Free ¹³CO₂ signal was not observed at 125 ppm, suggesting that CO₂ is not being physisorbed to any measureable extent in these IL samples but is only being chemisorbed.

The mass spectra of 1,2,3-triazolide IL solutions in methanol were all obtained, and the results are listed in Table 4. In all five cases, the molecular ion for the cations were observed in positive mode, and the molecular ion for the triazolide anions were observed in negative mode, confirming the identities of all products. In addition to the molecular ions, evidence of dimeric anion species was observed for all ILs except 4, which yielded a molecular ion signal. The reactive ring proton at C₅ is the most likely site for any side reactions which may be occurring, although the phosphonium α -methylene groups may also provide a reaction site.^{38,39}

These materials were further characterized by FTIR studies. Samples of ILs 1–5 were deposited as neat films on CaF₂ and were observed by transmission FTIR under varying pressures of CO₂. ILs 1–4 were first evacuated (<10⁻⁶ mbar), then dosed with 10 and 100 mbar CO₂, and new features were observed to appear in the carbamate regions of the spectrum (1100–1200, 1600–1800 cm⁻¹). It was not possible to prepare a sufficiently thin layer of 5 to obtain useful FTIR spectra. The spectra obtained for 2 are shown in Fig. 6, and new features can be seen to appear after 10 mbar CO₂ at 1754, 1628, and 1280 cm⁻¹ (see arrows). These features disappeared when the sample was again

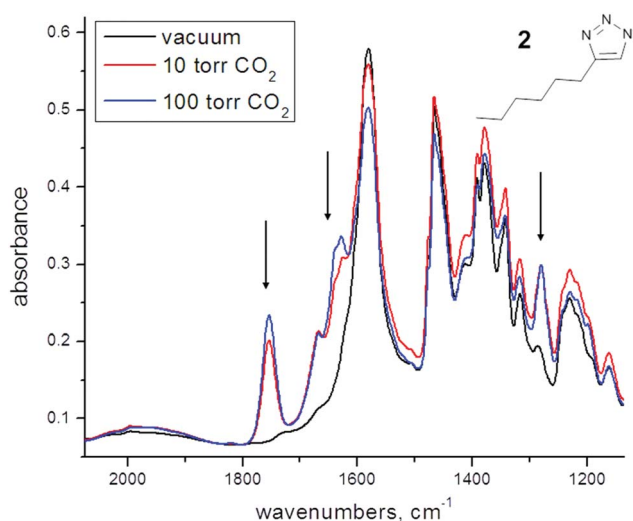


Fig. 6 Variable pressure FTIR spectra of 2 under vacuum and after exposure to 10 and 100 mbar CO₂ (carbamate bands indicated by arrows).



Fig. 7 1 in 2 mL water after 1 week under ambient conditions.

evacuated to 10⁻⁶ mbar, suggesting that, like other azolides, the CO₂ adsorption is reversible for triazolide ILs.¹¹ Similar spectra for 1, 3, and 4 (ESI Fig. 1–3†) in addition to the Raman spectra of untreated 1–4 (ESI Fig. 8–11†) were also collected.

Samples of dry 1–5 were treated with H₂O in an effort to probe their water stability. All of the triazolide ILs failed to dissolve in an excess of H₂O, even after 1 week. IL 4 was initially insoluble, but appeared to decompose after 2 days to give a purplish solution. The remaining ILs were stable and immiscible in H₂O for the duration of the experiment. Examination of the ¹H NMR spectra of 1–5 in D₂O failed to show any peaks besides those expected for the ILs, suggesting that the small amount of material that is dissolved is stable in water. A sample of 1 (0.5 g) which had been sitting in water (5 mL) for 1 week at ambient temperature is shown in Fig. 7, in which the insoluble IL can be seen at the lower left portion of the vial. Similar pictures of 2–5 are shown in ESI Fig. 4–7.†

Dissolving dry samples of 1–5 in D₂O for NMR analysis was also attempted, but failed to show any signal, suggesting that the ILs are insoluble in aqueous media. When sufficient CD₃OD was added to the D₂O solution to permit ¹H NMR signals to be observed, no changes from the starting IL NMR signals could be detected. This lack of change implies that, in addition to being insoluble, 1, 2, 3 and 5 do not tend to react with water; however, they are hygroscopic in nature and take up significant amounts of water.

Computational studies of the 1,2,3-triazolide system were used to calculate the expected anionic charge for the atoms in the azolide rings that were synthesized and the unsubstituted 1,2,3-triazolide anion. The results of these studies are illustrated in Fig. 8, and the charges are tabulated in ESI Table 7.† Due to the symmetry of the unsubstituted 1,2,3-triazolide anion, the charges on N₁ and N₃ are identical and roughly twice as large as that expected for the central N₂ atom. In the case of the asymmetric substituted 1,2,3-triazolide anions, the largest negative charge tended to be found at N₁ and the smallest at N₂; N₃ was the largest negative charge for 2 and 5. It was expected

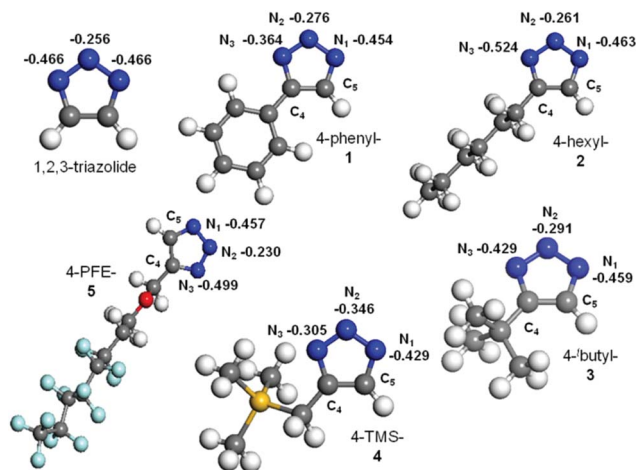


Fig. 8 Calculated CHELPG charges on N_1 through N_3 atoms for anions in ILs 1–5. C atoms are shown in grey, H in white, N in blue, Si in yellow, F in aqua, and O in red.

that the N atom with the largest negative charge would be the most energetically favorable location for interaction with either CO_2 or H_2O . This result for the anions diverged from theoretical work performed on the protonated 1,2,3-triazoles, where the N_2 tautomer tended to be the most stable.^{36,37}

Computational studies of the reaction of the 4-substituted 1,2,3-triazolide anions with CO_2 and H_2O were also conducted. The results of these studies suggest that H_2O interacts more strongly than CO_2 . In all cases, the N_1 atom was the site of the strongest interaction for both CO_2 and H_2O . For CO_2 , the N_2 and N_3 interaction energies varied from 60% to 90% of that found for the N_1 interaction. For H_2O , interaction energies tended not to vary much between N atoms. The calculated values for the interaction with CO_2 and H_2O are listed in ESI Tables 8 and 9,[†] respectively. An illustration of the interactions dealt with in these computations is shown in Fig. 9 for the anion of 2 interacting with CO_2 and H_2O , respectively. In the case of 2, N_3 had a larger negative charge than N_1 , but interaction energy with CO_2 and H_2O were still the greatest with N_1 .

In the unsubstituted 1,2,3-triazolide anion, the interaction energy with CO_2 was found to be -52 kJ mol^{-1} at N_1 , whereas the interaction with H_2O was -67 kJ mol^{-1} . In the absence of any azole ring substitution, H_2O interacts more strongly than CO_2 . These interactions are also reflected in the shorter bond distances calculated between CO_2 and the N_1 to N_3 atoms, as

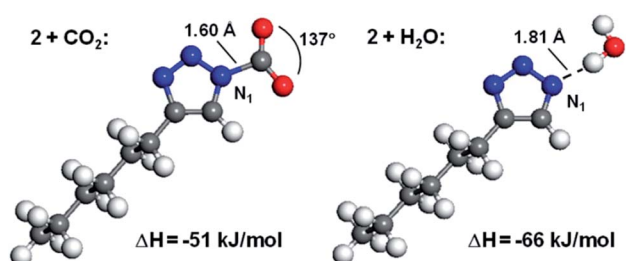


Fig. 9 Calculated interactions of anion of 2 with CO_2 and H_2O . The C atoms are shown in grey, H in white, N in blue, and O in red.

well as in the amount of bend angle induced in the reacting CO_2 molecule. The N–C bond distance at N_1 is 1.61 \AA , or 0.06 \AA shorter than the distance at N_2 ; the O–C–O bond angle when bonded to N_1 is 137° , or 3° less linear than when bonded at N_2 .

When the electronic effects of substitution at the 4-position are accounted for, the relative differences in interaction energies with both CO_2 and H_2O change considerably. In the phenyl anion of 1, CO_2 was found to have interaction energy at N_1 of -36 kJ mol^{-1} , and H_2O was found to have interaction energy of -61 kJ mol^{-1} . In the hexyl-substituted anion of 2, CO_2 was found to have interaction energy at N_1 of -51 kJ mol^{-1} , and H_2O was found to have interaction energy of -66 kJ mol^{-1} . The effect of replacing an electron withdrawing substituent (1 – phenyl) at the 4-position of the azole ring with an electron donating group (2 – hexyl) was to strengthen the interaction for both CO_2 and H_2O , but the relative difference in energy was greater for CO_2 than it was for H_2O . This same trend is observed in all substituted versions of the 1,2,3-triazolide anion studied (1–5).

These interactions are consistent with the expectation that the electron withdrawal of the phenyl group in 1 pulls negative charge away from the triazolide N atoms, rendering them less able to chemically interact with CO_2 or H_2O . Conversely, the electron donation from the hexyl group in 2 increases the negative charges on the triazolide N atoms and renders them more active towards both CO_2 and H_2O .

Conclusions

This study highlights the importance of selecting the right substituent and points to the fact that the reactivity can be altered based upon the electronic nature and steric bulk of the substituents. In this work, we have systematically studied the effects of electron donating/withdrawing groups and steric hindrance on the CO_2 uptake behaviour and interactions with water of triazolide-based AHA ILs. The absorption capacities of the materials in this study, $0.07\text{--}0.40 \text{ mol CO}_2$ per mol IL, were highly dependent upon the nature of side groups present. We found that electron donating groups are generally more desirable for CO_2 uptake.

Characterization of the CO_2 -reacted products by ^{13}C NMR showed the formation of multiple isomers of carbamates. While the AHA ILs were not water soluble, the presence of even small amounts of moisture in the ILs exerted a large influence on both the viscosity and physical state of the IL after CO_2 absorption, indicating that caution must be taken when comparing physical properties of different ILs. Computational studies of the triazolide anions suggest that they should be more reactive towards water than CO_2 and that the N_1 atom of the azole ring should provide the most reactive site for CO_2 . However, the presence of water does not alter the overall CO_2 uptake. One explanation may be that in the presence of water the CO_2 reaction happens *via* an alternate mechanism involving bicarbonate formation.

Acknowledgements

This project was funded by the Department of Energy, National Energy Technology Laboratory, an agency of the United States Government, through a support contract with URS

Energy & Construction, Inc. Neither the United States Government nor any agency thereof, nor any of their employees, nor URS Energy & Construction, Inc., nor any of their employees, makes any warranty, expressed or implied, or assumes any legal liability or responsibility for the accuracy, completeness, or usefulness of any information, apparatus, product, or process disclosed, or represents that its use would not infringe privately owned rights. Reference herein to any specific commercial product, process, or service by trade name, trademark, manufacturer, or otherwise, does not necessarily constitute or imply its endorsement, recommendation, or favoring by the United States Government or any agency thereof. The views and opinions of authors expressed herein do not necessarily state or reflect those of the United States Government or any agency thereof.

Notes and references

- 1 T. W. P. Wasserscheid, *Ionic Liquids in Synthesis*, Wiley, Weinheim, 2003.
- 2 C. Wu, T. P. Senftle and W. F. Schneider, *Phys. Chem. Chem. Phys.*, 2012, **14**, 13163–13170.
- 3 N. MacDowell, N. Florin, A. Buchard, J. Hallett, A. Galindo, G. Jackson, C. S. Adjiman, C. K. Williams, N. Shah and P. Fennell, *Energy Environ. Sci.*, 2010, **3**, 1645–1669.
- 4 F. Karadas, M. Atilhan and S. Aparicio, *Energy Fuels*, 2010, **24**, 5817–5828.
- 5 M. Hasib-ur-Rahman, M. Siaj and F. Larachi, *Chem. Eng. Process.*, 2010, **49**, 313–322.
- 6 J. E. Bara, D. E. Camper, D. L. Gin and R. D. Noble, *Acc. Chem. Res.*, 2010, **43**, 152–159.
- 7 M. Petkovic, K. R. Seddon, L. P. Rebelo and C. Silva Pereira, *Chem. Soc. Rev.*, 2011, **40**, 1383–1403.
- 8 H. B. Nulwala, C. N. Tang, B. W. Kail, K. Damodaran, P. Kaur, S. Wickramanayake, W. Shi and D. R. Luebke, *Green Chem.*, 2011, **13**, 3345–3349.
- 9 B. F. Goodrich, J. C. de la Fuente, B. E. Gurkan, Z. K. Lopez, E. A. Price, Y. Huang and J. F. Brennecke, *J. Phys. Chem. B*, 2011, **115**, 9140–9150.
- 10 R. L. Thompson, K. Damodaran, D. Luebke and H. Nulwala, *Synlett*, 2013, **24**, 1093–1096.
- 11 C. Wang, X. Luo, H. Luo, D. E. Jiang, H. Li and S. Dai, *Angew. Chem., Int. Ed. Engl.*, 2011, **50**, 4918–4922.
- 12 B. Gurkan, B. F. Goodrich, E. M. Mindrup, L. E. Ficke, M. Massel, S. Seo, T. P. Senftle, H. Wu, M. F. Glaser, J. K. Shah, E. J. Maginn, J. F. Brennecke and W. F. Schneider, *J. Phys. Chem. Lett.*, 2010, **1**, 3494–3499.
- 13 H. C. Kolb, M. G. Finn and K. B. Sharpless, *Angew. Chem., Int. Ed. Engl.*, 2001, **40**, 2004–2021.
- 14 B. E. Gurkan, T. R. Gohndrone, M. J. McCready and J. F. Brennecke, *Phys. Chem. Chem. Phys.*, 2013, **15**, 7796–7811.
- 15 C. W. Tornøe, C. Christensen and M. Meldal, *J. Org. Chem.*, 2002, **67**, 3057–3064.
- 16 J. H. Davis, *Chem. Lett.*, 2004, **33**, 1072–1077.
- 17 M. Ramdin, T. W. de Loos and T. J. H. Vlugt, *Ind. Eng. Chem. Res.*, 2012, **51**, 8149–8177.
- 18 E. D. Bates, R. D. Mayton, I. Ntai and J. H. Davis, *J. Am. Chem. Soc.*, 2002, **124**, 926–927.
- 19 G. K. Cui, J. J. Zheng, X. Y. Luo, W. J. Lin, F. Ding, H. R. Li and C. M. Wang, *Angew. Chem., Int. Ed.*, 2013, **52**, 10620–10624.
- 20 C. M. Wang, H. M. Luo, H. R. Li, X. Zhu, B. Yu and S. Dai, *Chem. – Eur. J.*, 2012, **18**, 2153–2160.
- 21 D. V. Francis, D. H. Miles, A. I. Mohammed, R. W. Read and X. B. Wang, *J. Fluorine Chem.*, 2011, **132**, 898–906.
- 22 C. M. White, B. R. Strazisar, E. J. Granite, J. S. Hoffman and H. W. Pennline, *J. Air Waste Manag. Assoc.*, 2003, **53**, 645–715.
- 23 H. Tang and C. Wu, *ChemSusChem*, 2013, **6**, 1050–1056.
- 24 J. Ren, L. Wu and B.-G. Li, *Ind. Eng. Chem. Res.*, 2013, **52**, 8565–8570.
- 25 F. G. Bordwell, *Acc. Chem. Res.*, 1988, **21**, 456–463.
- 26 E. W. Lemmon and R. Tillner-Roth, *Fluid Phase Equilib.*, 1999, **165**, 1–21.
- 27 E. W. Lemmon, A. P. Peskin, M. O. McLinden and D. G. Friend, NIST Standard Reference Database 12; Thermodynamic and Transport Properties of Pure Fluids, 2000.
- 28 C. M. Breneman and K. B. Wiberg, *J. Comput. Chem.*, 1990, **11**, 361–373.
- 29 G. W. T. M. J. Frisch, H. B. Schlegel, G. E. Scuseria, M. A. Robb, J. R. Cheeseman, G. Scalmani, V. Barone, B. Mennucci, G. A. Petersson, H. Nakatsuji, M. Caricato, X. Li, H. P. Hratchian, A. F. Izmaylov, J. Bloino, G. Zheng, J. L. Sonnenberg, M. Hada, M. Ehara, K. Toyota, R. Fukuda, J. Hasegawa, M. Ishida, T. Nakajima, Y. Honda, O. Kitao, H. Nakai, T. Vreven, J. A. Montgomery, Jr., J. E. Peralta, F. Ogliaro, M. Bearpark, J. J. Heyd, E. Brothers, K. N. Kudin, V. N. Staroverov, R. Kobayashi, J. Normand, K. Raghavachari, A. Rendell, J. C. Burant, S. S. Iyengar, J. Tomasi, M. Cossi, N. Rega, J. M. Millam, M. Klene, J. E. Knox, J. B. Cross, V. Bakken, C. Adamo, J. Jaramillo, R. Gomperts, R. E. Stratmann, O. Yazyev, A. J. Austin, R. Cammi, C. Pomelli, J. W. Ochterski, R. L. Martin, K. Morokuma, V. G. Zakrzewski, G. A. Voth, P. Salvador, J. J. Dannenberg, A. D. S. Dapprich, Ö. Daniels, O. Farkas, J. B. Foresman, J. V. Ortiz, J. Cioslowski and D. J. Fox, *Gaussian 09, Revision A.1*, Gaussian, Inc., Wallingford, CT, 2009.
- 30 C. Maton, N. De Vos and C. V. Stevens, *Chem. Soc. Rev.*, 2013, **42**, 5963–5977.
- 31 S. N. V. K. Aki, B. R. Mellein, E. M. Saurer and J. F. Brennecke, *J. Phys. Chem. B*, 2004, **108**, 20355–20365.
- 32 A. Yokozeki, M. B. Shiflett, C. P. Junk, L. M. Grieco and T. Foo, *J. Phys. Chem. Soc. B*, 2008, **112**, 16654–16663.
- 33 C. A. Tolman, *Chem. Rev.*, 1977, **77**, 313–348.
- 34 W. Shi, K. Damodaran, H. B. Nulwala and D. R. Luebke, *Phys. Chem. Chem. Phys.*, 2012, **14**, 15897–15908.
- 35 W. Shi, C. R. Myers, D. R. Luebke, J. A. Steckel and D. C. Sorescu, *J. Phys. Chem. B*, 2012, **116**, 283–295.
- 36 W. P. Ozimiński, J. C. Dobrowolski and A. P. Mazurek, *J. Mol. Struct.*, 2003, **651–653**, 697–704.
- 37 H. A. Dabbagh, E. Rasti and A. N. Chermahini, *J. Mol. Struct.: THEOCHEM*, 2010, **947**, 92–100.
- 38 T. Ramnial, D. D. Ino and J. A. Clyburne, *Chem. Commun.*, 2005, 325–327.
- 39 T. Ramnial, S. A. Taylor, M. L. Bender, B. Gorodetsky, P. T. Lee, D. A. Dickie, B. M. McCollum, C. C. Pye, C. J. Walsby and J. A. Clyburne, *J. Org. Chem.*, 2008, **73**, 801–812.